JOURNAL OF BACTERIOLOGY, Mar. 2008, p. 2221–2226 Vol. 190, No. 6
0021-9193/08/$08.00+0 doi:10.1128/JB.01753-07
Copyright © 2008, American Society for Microbiology. All Rights Reserved.

Identification of Amino Acid Residues within the N-Terminal Domain of EspA That Play a Role in EspA Filament Biogenesis and Function▽

Mona P. Singh, Robert K. Shaw, Stuart Knutton, Mark J. Pallen, Valerie F. Crepin, and Gad Frankel*

Division of Cell and Molecular Biology, Imperial College, London SW7 2AZ, United Kingdom, and Division of Immunity and Infection, School of Medicine, University of Birmingham, Birmingham B15 2TT, United Kingdom

Received 1 November 2007/Accepted 23 December 2007

Enteropathogenic *Escherichia coli* employs a filamentous type III secretion system, made by homopolymerization of the translocator protein EspA. In this study, we have shown that the N-terminal region of EspA has a role in EspA's protein stability, interaction with the CesAB chaperone, and filament biogenesis and function.

Type III secretion systems (T3SSs) are complex multiprotein assemblies that export proteins from the bacterial cytoplasm to the exterior without a periplasmic intermediate (10, 24). T3SSs are employed in two functional contexts: the translocation of bacterial effector proteins into eukaryotic cells and flagellar protein export. These two different types of T3SSs share a conserved core set of homologous proteins, which include the ATPase that powers secretion and components of the apparatus spanning the cell envelope (9, 24). In both cases, the secretion system is woven into a larger apparatus that includes a hollow, filamentous organelle, which comprises, in the case of the flagellum, the flagellar hook and filament, and in the case of nonflagellar systems, the needle and the translocon (10, 19).

Three bacterial gastrointestinal pathogens—enterohemorrhagic *Escherichia coli*, enteropathogenic *E. coli* (EPEC) (reviewed in reference 12), and *Citrobacter rodentium* (reviewed in reference 22)—exploit a T3SS encoded by the pathogenicity island known as the locus for enterocyte effacement (LEE) (20) to colonize the gut mucosa via attaching and effacing lesion formation (15). The LEE-encoded T3SS is unusual in that it possesses a hollow filamentous extension, the EspA filament (7, 16), which connects the EscF needle to the putative translocation pore in the eukaryotic plasma membrane believed to be composed of the translocator proteins EspB and EspD (reviewed in reference 11). Effectors are believed to be passed through a channel within the EspA filament during their translocation into host cells (4, 6), leading in this system to actin polymerization at the site of bacterial attachment (reviewed in reference 11), which can be detected by the fluorescent actin staining (FAS) test (14).

Several similarities between the EspA filament (with an outer diameter of ~120 Å and an inner central channel diameter of ~25 Å) (6) and the flagellar filament (with an outer diameter of ~240 Å and an inner central channel diameter of ~20 Å) (28) hint at a common ancestry, including related filament structures (similar helical symmetries and packings) and identical modes of polymerization (elongation at the filament tip) (4, 29). Limited sequence similarity, detectable by BLAST searches, between the C terminus of EspA and some flagellins is also suggestive of homology (23). Furthermore, structural, sequence-based, and functional investigations suggest that EspA has a domain structure similar to that of flagellin, with N- and C-terminal coiled-coil domains and a variable, central, surface-exposed domain (5, 6, 16, 23, 27, 28).

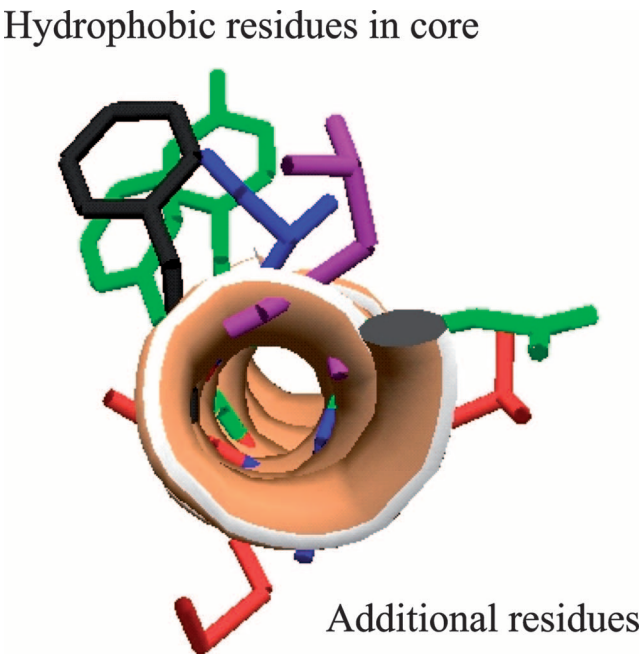

FIG. 1. Residues from the N-terminal domain of EspA mutated in this study. Shown are the residues that form the hydrophobic core of the EspA-CesAB complex (L39, F42, I46, F49, and Y53) and the additional residues from this domain that were targeted for mutagenesis (Q43, A44, A45, L47, and M48). Purple, hydrophobic-core wild-type phenotype; red, noncore wild-type phenotype; green, vestigial EspA filaments; blue, no filaments/FAS positive; black, no filaments/FAS negative (as in Fig. 2).

In flagellin, an intrasubunit coiled-coil interaction between the N- and C-terminal domains is a prerequisite for the protein's polymerization into the flagellar filament (21, 28). Building on the analogy with flagellin, we have already shown that alterations in the C-terminal coiled-coil domain of EspA interfere with the formation of typical EspA filaments (8). The

* Corresponding author. Mailing address: Division of Molecular and Cellular Biology, Flowers Building, Imperial College London, London SW7 2AZ, United Kingdom. Phone: 44 020 2594 5253. Fax: 44 020 5794 3069. E-mail: g.frankel@imperial.ac.uk.

▽ Published ahead of print on 4 January 2008.

Downloaded from http://jb.asm.org/ on May 15, 2021 by guest

TABLE 1. Strains and plasmids used in this study

Strain or plasmid	Relevant features	Reference or source	Primers used[b]
Strain			
E2348/69	Wild-type EPEC O127:H6	17	
UMD872	E2348/69Δ*espA*::*aphA3*	13	
DF1358	E2348/69Δ*cesAB*	3	
Plasmid			
pSA10	pKK177-3 derivative containing the *lacI*^{q} gene	25	NA
pET28a	Expressing vector	Novagen	NA
pICC285	pSA10 wild-type expressing EspA	4	EspA-Fw1 and EspA-Rv1
pICC369[a]	pSA10 expressing EspA(Leu39Arg)	This study	EspAL39R-Fw, EspAL39R-Rv
pICC370[a]	pSA10 expressing EspA(Phe42Arg)	This study	EspAF42R-Fw, EspAF42R-Rv
pICC371	pSA10 expressing EspA(Glu43Arg)	This study	EspA-Fw1 and EspAQ43R-Rv, EspAQ43R-Fw and EspA-Rv1
pICC372	pSA10 expressing EspA(Ala44Arg)	This study	EspA-Fw1 and EspAA44R-Rv, EspAA44R-Fw and EspA-Rv1
pICC373	pSA10 expressing EspA(Ala45Arg)	This study	EspA-Fw1 and EspAA45R-Rv, EspAA45-Fw and EspA-Rv1
pICC374[a]	pSA10 expressing EspA(Ile46Arg)	This study	EspAI46R-Fw, EspAI46R-Rv
pICC375	pSA10 expressing EspA(Leu47Arg)	This study	EspA-Fw1 and EspAL47R-Rv, EspAL47R-Fw and EspA-Rv1
pICC376	pSA10 expressing EspA(Met48Arg)	This study	EspA-Fw1 and EspAM48R-Rv, EspAM48R-Fw and EspA-Rv1
pICC377	pSA10 expressing EspA(Phe49Arg)	This study	EspA-Fw1 and EspAF49R-Rv, EspAF49R-Fw and EspA-Rv1
pICC378	pSA10 expressing EspA(Tyr53Arg)	This study	EspA-Fw1 and EspAY53R-Rv, EspAY53R-Fw and EspA-Rv1
pICC379	pET28a expressing EspA and CesAB-His_6	This study	EspA-Fw2 and EspA-Rv2, CesAB-Fw and CesAB-Rv
pICC380	pET28a expressing EspA(Leu39Arg) and CesAB-His_6	This study	EspA-Fw2 and EspA-Rv2, CesAB-Fw and CesAB-Rv
pICC381	pET28a expressing EspA(Phe42Arg) and CesAB-His_6	This study	EspA-Fw2 and EspA-Rv2, CesAB-Fw and CesAB-Rv
pICC382	pET28a expressing EspA(Ile46Arg) and CesAB-His_6	This study	EspA-Fw2 and EspA-Rv2, CesAB-Fw and CesAB-Rv
pICC383	pET28a expressing EspA(Phe49Arg) and CesAB-His_6	This study	EspA-Fw2 and EspA-Rv2, CesAB-Fw and CesAB-Rv
pICC384	pSA10 expressing EspA-His_6	This study	EspA-Fw1 and EspA-Rv3
pICC385	pSA10 expressing EspA(Leu39Arg)-His_6	This study	EspA-Fw1 and EspA-Rv3
pICC424	pSA10 expressing EspA(Phe42Arg)-His_6	This study	EspA-Fw1 and EspA-Rv3
pICC425	pSA10 expressing EspA(Ile46Arg)-His_6	This study	EspA-Fw1 and EspA-Rv3
pICC426	pSA10 expressing EspA(Phe49Arg)-His_6	This study	EspA-Fw1 and EspA-Rv3

[a] Mutations were introduced by QuikChange.
[b] NA, not applicable.

recently determined structure of monomeric EspA in a complex with its chaperone, CesAB, reveals that these two proteins form a four-helix bundle, with a hydrophobic core fashioned from coiled-coil interactions involving the C- and N-terminal domains of EspA (27). CesAB is essential for stabilizing EspA in the bacterial cytosol, EspA protein secretion, and EspA filament biogenesis (3). The aim of this study was to extend our previous work on the C-terminal region (8) to the N-terminal domain of EspA.

The N-terminal EspA domain is predicted with low probability to be a coiled coil. For this reason, amino acids in the heptad repeat of coiled coils were manually assigned positions a-b-c-d-e-f-g, where the a and d residues are largely hydrophobic and form the hydrophobic core (18). In order to investigate

TABLE 2. Nucleotide sequences for the primers used in this study

Primer	Nucleotide sequence[a]
EspAL39R-Fw	5′-GTT ATT GAT CTA TTT AAT AAA CGC GGT GTT TTT CAG GCT GCA ATT C
EspAL39R-Rv	5′-AAT TGC AGC CTG AAA AAC ACC GCG TTT ATT AAA TAG ATC AAT AAC
EspAF42R-Fw	5′-CTA TTT AAT AAA CTC GGT GTT CGT CAG GCT GCA ATT CTC ATG
EspAF42R-Rv	5′-CAT GAG AAT TGC AGC CTG ACG AAC ACC GAG TTT ATT AAA TAG
EspAQ43R-Fw	5′-GGT GTT TTT CGC GCT GCA ATT CTC ATG TTT GCC TAT ATG
EspAQ43R-Rv	5′-AAT TGC AGC GCG AAA AAC ACC GAG TTT ATT AAA TAG
EspAA44R-Fw	5′-GTT TTT CAG CGT GCA ATT CTC ATG TTT GCC TAT ATG TAT C
EspAA44R-Rv	5′-GAG AAT TGC ACG CTG AAA AAC ACC GAG TTT ATT AAA TAG
EspAA45R-Fw	5′-GTT TTT CAG GCT CGA ATT CTC ATG TTT GCC TAT ATG TAT CAG
EspAA45R-Rv	5′-CAT GAG AAT TCG AGC CTG AAA AAC ACC GAG TTT ATT AAA TAG
EspAI46R-Fw	5′-GGT GTT TTT CAG GCT GCA CGT CTC ATG TTT GCC TAT ATG
EspAI46R-Rv	5′-CAT ATA GGC AAA CAT GAG ACG TGC AGC CTG AAA AAC ACC
EspAL47R-Fw	5′-GCT GCA ATT CGT ATG TTT GCC TAT ATG TAT CAG GCA C
EspAL47R-Rv	5′-GGC AAA CAT ACG AAT TGC AGC CTG AAA AAC ACC GAG
EspAM48R-Fw	5′-GCA ATT CTC CGG TTT GCC TAT ATG TAT CAG GCA CAA
EspAM48R-Rv	5′-ATA GGC AAA CCG GAG AAT TGC AGC CTG AAA AAC ACC
EspAF49R-Fw	5′-ATT CTC ATG CGT GCC TAT ATG TAT CAG GCA CAA AGC
EspAF49-Rv	5′-CAT ATA GGC ACG CAT GAG AAT TGC AGC CTG AAA AAC
EspAY53-Fw	5′-CTC ATG TTT GCC TAT ATG CGT CAG GCA CAA AGC GAT CTG
EspAY53-Rv	5′-CAG ATC GCT TTG TGC CTG ACG CAT ATA GGC AAA CAT GAG
EspA-Fw1	5′-CG**G AAT TC**A TGG ATA CAT CAACTA CAG C
EspA-Fw2	5′-CAT G**CC ATG G**AT ACA TCA ACT ACA GCA TCA GTT GC
EspA-Rv1	5′-TTT **TCT GCA G**TT ATT TAC CAA GGG ATA TTC C
EspA-Rv2	5′-CGC **GGA TCC** TTA TTT ACC AAG GGA TAT TCC TG
EspA-Rv3	5′-AAA **ACT GCA G**TT AGT GAT GGT GAT GGT GAT GTT TAC CAA GGG ATA TTC CTG
CesAB-Fw	5′-CG**G AAT TC**G GTA CTA TT TTC TAT TAT TTC TAT TCC
CesAB-Rv	5′-CG**G GAT CC**T TTA AGA AGG AGA TAT ACA TAT GAG TAT TGT GAG CCA AACAAG

[a] Restriction sites are in bold, and mutated base pairs are underlined.

Downloaded from http://jb.asm.org/ on May 15, 2021 by guest

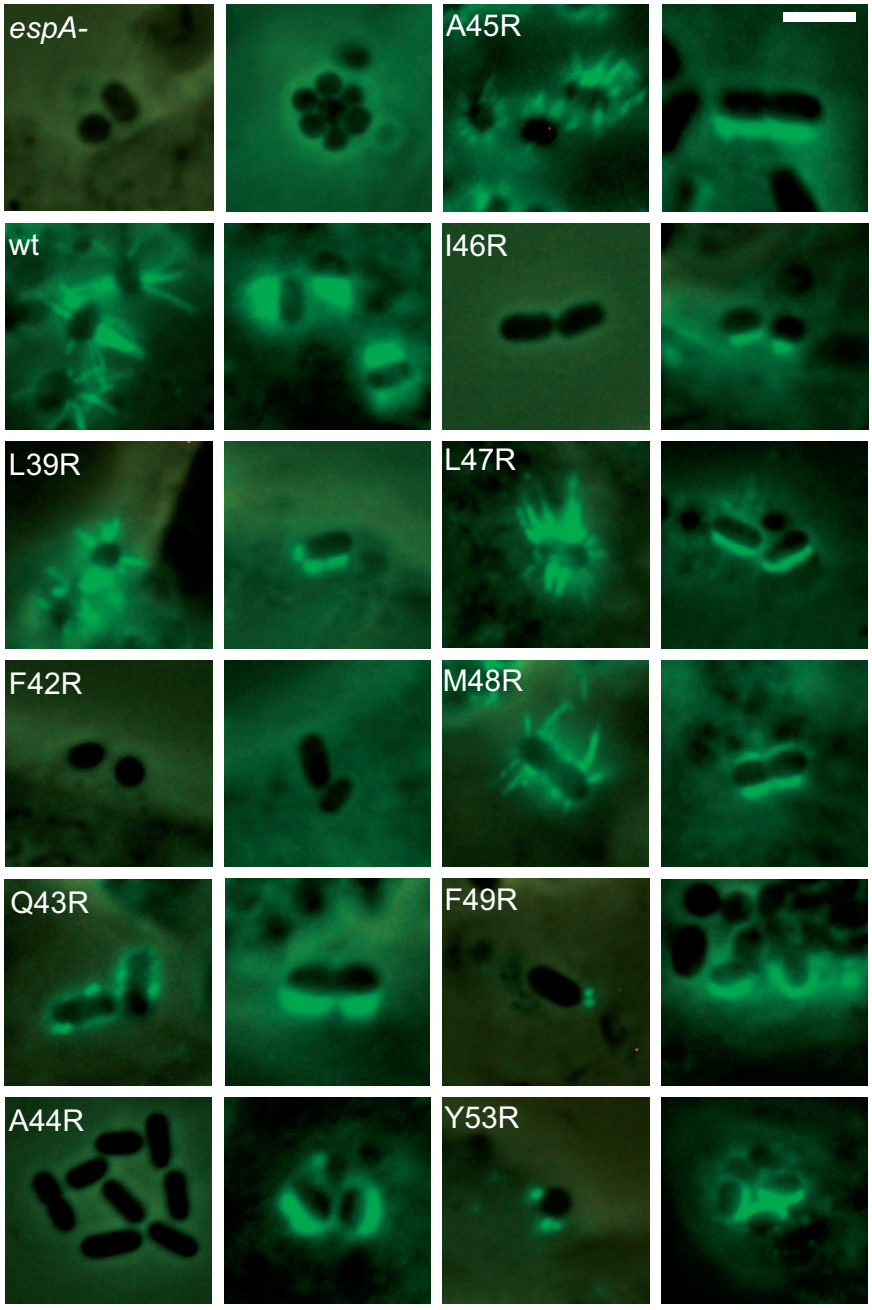

FIG. 2. EspA filaments and fluorescent actin staining. HeLa cells were infected with LB-grown EPECΔ*espA* (UMD872) expressing EspA N-terminal mutants. wt, wild type. Scale bar = 0.2 μm.

whether the N-terminal domain of EspA plays a role in EspA filament biogenesis and function, we selected the nonpolar residues L39, F42, I46, F49, and Y53, which are predicted to occupy positions a and d of the heptad repeat; residues L47 and M48, which are predicted to lie at position c of the heptad coiled-coil repeat and to be orientated away from the hydrophobic core and exposed to the external environment; and amino acids Q43, A44, and A45 (Fig. 1) for substitution with arginine (which is predicted to disrupt coiled-coil domain interactions). Site-directed mutagenesis was performed using the QuikChange site-directed mutagenesis kit (Stratagene), by following the manufacturer's instructions and procedures described previously (8), or overlapping PCR as described before (4) using pICC285 carrying the wild-type *espA* gene of EPEC strain E2348/69 as a template (Table 1). Oligonucleotide pairs used for mutagenesis are shown in Tables 1 and 2. The correct incorporation of each mutation was verified by DNA sequencing. The constructs were transformed into strain UMD872 (EPECΔ*espA*) (13) for analysis of the phenotypic effects.

We used immunofluorescence with an anti-EspA antibody to determine whether mutated EspA could assemble filaments on the bacterial cell surface during a conventional 3-h infection

Downloaded from http://jb.asm.org/ on May 15, 2021 by guest

of HeLa cells, as described previously (2, 8). Briefly, subconfluent monolayers of HeLa cells, grown on glass coverslips as described previously (16), were infected for 3 h with a 1:100 dilution of an overnight LB culture in the presence of 1 mM IPTG (isopropyl-β-D-thiogalactopyranoside). Nonadherent bacteria were removed, and the cells were fixed with 4% formalin for 20 min and incubated for 45 min with rabbit EPEC EspA polyclonal antiserum diluted 1:100 as described previously (16). Following three washes, the EspA filaments were labeled for 45 min with a 1:100 goat anti-rabbit antibody–Alexa 488 fluorescence conjugate (Molecular Probes) (16). Coverslips were mounted and examined on a Leica DMRE microscope.

Filaments formed by EspA(L39R), EspA(A45R), EspA(L47R), and EspA(M48R) were indistinguishable from the wild-type EspA filaments. EspA(Q43R), EspA(F49R), and EspA(Y53R) produced stumpy, vestigial filaments, similar to those seen with substitutions affecting hydrophobic residues in the C-terminal coiled-coil domain of EspA (8). Strains expressing EspA(F42R), EspA(A44R), and EspA(I46R) produced no visible filaments (Fig. 2).

We next employed the FAS test (14) as a marker for functional EspA filaments and effector protein translocation. Cellular actin was stained following cell membrane permeabilization with a 5-μg/ml solution of phalloidin-fluorescein isothiocyanate (Sigma). All strains capable of forming filaments (wild-type and vestigial morphologies) were FAS positive (Fig. 2). UMD872 expressing EspA(F42R), which did not produce EspA filaments, was FAS negative (Fig. 2). The most puzzling result was that while no EspA(A44R) or EspA(I46R) filaments were detected, UMD872 expressing these EspA derivatives were able to translocate effector proteins that trigger actin polymerization, as measured by the FAS test (Fig. 2).

In order to determine if the induction of LEE gene expression might have an impact on the ability to detect EspA filaments on UMD872 expressing EspA(F42R), EspA(A44R), or EspA(I46R), we infected HeLa cells with bacteria preincubated for 3 h in Dulbecco's modified Eagle's medium in a 5% CO_2 atmosphere, which are established LEE-inducing conditions (1). EspA staining was performed 30, 60, and 90 min postinfection. This revealed that while vestigial EspA filaments were seen on 5% of the UMD872 bacteria expressing EspA(I46R) at 30 and 60 min, somewhat longer EspA filaments were seen on 30% of the adherent bacteria at 90 min postinfection (Fig. 3). In contrast, vestigial EspA filaments were seen at all time points on 5% of adherent UMD872 bacteria expressing EspA(A44R), while only punctuated staining was seen on <5% of adherent UMD872 bacteria expressing EspA(F42R) (Fig. 3). These results suggest that EspA(F42R), the only derivative with a mutation that resulted in FAS-negative staining, is the least stable of all the EspA mutants, followed by EspA(A44R) and EspA(I46R), and that the preactivation of LEE gene expression appears to stabilize mutant EspA filaments; the mechanism involved in this phenomenon is unknown.

We next analyzed preparations of whole-cell extracts and secreted EPEC proteins by Western blotting using polyclonal rabbit EPEC EspA antibody, as previously described (8). Western blotting of the bacterial cell pellets revealed that all mutant forms of EspA were expressed at similar levels (data not shown). Although secreted EspA is unstable and gives rise to multiple degradation products, the levels of such products detected in the supernatant were comparable for the mutants and wild-type EspA (Fig. 4A).

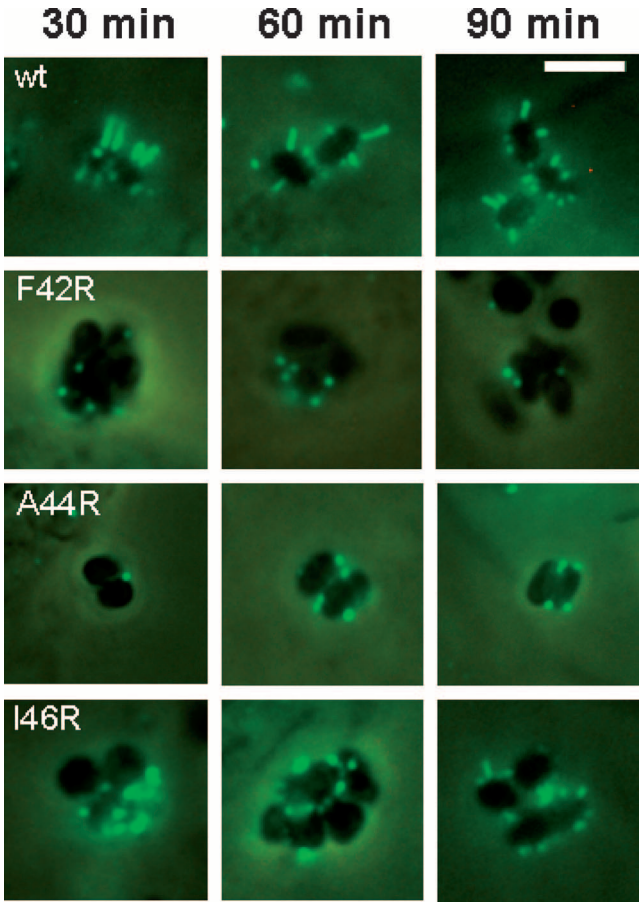

FIG. 3. EspA filament staining. HeLa cells were infected with primed EPEC Δ*espA* (UMD872) expressing selected EspA N-terminal mutants. wt, wild type. Scale bar = 0.2 μm.

We selected representative EspA mutants, elaborating filaments of wild-type morphology [EspA(L39R)], vestigial EspA filaments [EspA(F49R)], unstable EspA filaments [EspA(I46R)], and no EspA filaments [EspA(F42R)], for further studies of EspA protein secretion, stability, and interaction with the CesAB chaperone. To this end, we created synthetic operons consisting of a wild-type or mutant *espA* gene followed by a *cesAB* gene equipped with its own ribosome-binding site and a C-terminal His tag (Table 1) as previously described (26). *espA* was PCR amplified using pICC285 or a mutated vector as a template and primer pair EspA-Fw2 and EspA-Rv2 (Table 2). The PCR product was NcoI/BamHI digested and ligated into NcoI/BamHI-digested pET28a. *cesAB* was PCR amplified using a genomic E2348/69 DNA template and primer pair CesAB-Fw and CesAB-Rv (Table 2). Following BamHI/EcoRI digestion, the PCR product was ligated into pET28-a_EspA. Constructs were checked by DNA sequencing before transformation into *E. coli* BL21(DE3)/pLysS for protein expression as previously described (3). Each experiment was done at least twice. Western blotting revealed comparable

Downloaded from http://jb.asm.org/ on May 15, 2021 by guest

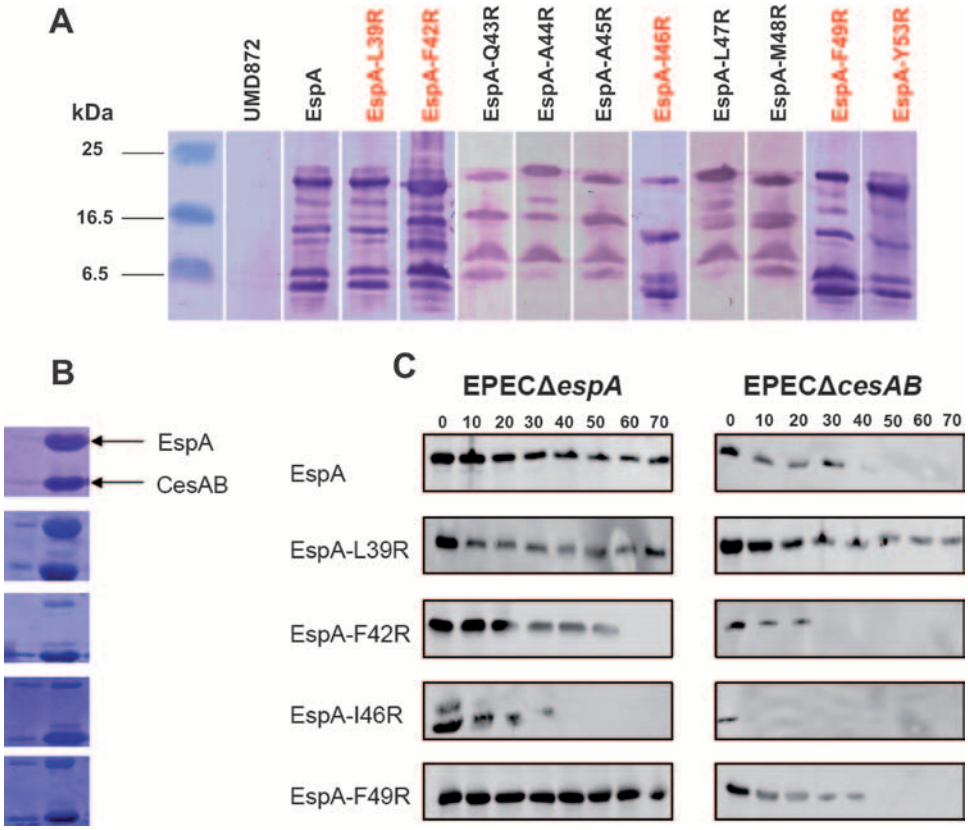

FIG. 4. (A) Detection of EspA N-terminal mutants in EPEC culture supernatants. Secreted EspA is highly unstable. Secretion profiles of EspA coiled-coil mutants are labeled in red. No EspA or background staining is seen in lane 1, which was loaded with the supernatant of EPEC Δ*espA*. (B) Coelution of EspA N-terminal mutants with His_6-tagged CesAB after affinity chromatography. (C) The stability of EspA N-terminal mutants in EPEC Δ*espA* (UMD872) and EPEC Δ*cesAB* (DF1358) was determined over time after protein synthesis was blocked by the addition of chloramphenicol.

levels of EspA and CesAB in bacterial cell extracts expressing each of the synthetic operons (data not shown). Nickel affinity purification, performed as previously described (26), revealed that coelution of EspA(L39R) with CesAB was unchanged compared to that of wild-type EspA (Fig. 4B), while EspA(F49R) showed an intermediate level of coelution and EspA(I46R) and EspA(F42R) showed reduced coelution (Fig. 4B).

We next determined whether the mutations affected the stability of cytosolic EspA in the presence or absence of CesAB. To this end, pICC285 and a plasmid encoding single-amino-acid EspA mutants were used as templates to amplify the *espA* gene, using primer pair EspA-Fw1 and EspA-Rv3 incorporating a His_6 carboxy-terminal tag (Table 1). The plasmids encoding wild-type and mutant EspAs were transformed into the UMD872 (Δ*espA*) and DF1358 (Δ*cesAB*) (3) strains. Analysis of the stability of the EspA mutants was performed as described previously (3). Briefly, bacteria were grown overnight in LB, diluted 1:50 in Dulbecco's modified Eagle's medium (LEE-inducing conditions), and incubated until an optical density at 600 nm of 0.35 was achieved, when 1 mM IPTG was added to induce EspA expression. The cultures were incubated for a further 30 min, followed by the addition of 200 μg/ml chloramphenicol to stop protein synthesis. The samples were analyzed by Western blotting using anti-His monoclonal antibodies (Oncogene), followed by an anti-mouse IgG–horseradish peroxidase conjugate and ECL detection reagents (Amersham). Each experiment was done at least twice.

Despite the fact that EspA was expressed from a high-copy-number plasmid, whereas *cesAB* was present in only one chromosomal copy, the level of wild-type EspA remained roughly constant for the duration of the experiment, while, in the absence of CesAB, wild-type EspA was rapidly degraded within 30 min of the addition of chloramphenicol (Fig. 4C). The stability of EspA(F49R) was similar to that of native EspA in the presence or absence of CesAB. By contrast, EspA(F42R) and, to a greater degree, EspA(I46R) were degraded more rapidly than wild-type EspA in the presence of CesAB, an effect that was even more marked in the absence of the chaperone. Curiously, EspA(L39R) was more stable than native EspA in the absence of CesAB (Fig. 4C).

The EspA filament and the flagellum are believed to have evolved from a common ancestor and share many homologous features, encompassing their three-dimensional structure, helical symmetry, ability to secrete effector proteins through their respective secretion apparatuses, and polarity of filament elongation. Although flagellin and EspA do not share identity at the amino acid level, the C-terminal coiled-coil domain of flagellin shows homology with the C-terminal coiled-coil domain of EspA (8, 24). We have shown previously that mutations in this region drastically impair EspA filament biogenesis (8). The crystal structure of the EspA-CesAB complex indi-

Downloaded from http://jb.asm.org/ on May 15, 2021 by guest

cated that EspA also has an N-terminal coiled-coil domain (27). In this study, we assessed the contribution of the N-terminal EspA domain, which encompasses the coiled-coil region, to EspA subunit stability and interaction with CesAB and EspA filament biogenesis and function. This revealed that residues within the N-terminal region have a role in chaperone interaction and protein stability. Although vestigial EspA filaments were produced by several EspA mutants, this did not impair their ability to translocate effector proteins into cultured HeLa cells; nonetheless, it is likely that only full-length EspA filaments can translocate effectors during infection of mucosal surfaces which are overlaid with thick mucus and glycocalyx protective layers.

That mutation of hydrophobic residues in both the EspA N-terminal (this study) and C-terminal (8) coiled domains produces similar EspA filament phenotypes is consistent with the hypothesis that an interaction between these two domains is required for EspA filament biogenesis. Indeed our preliminary data are indicative of an intramolecular coiled-coil interaction between the amino and carboxy coiled-coil EspA domains in a manner similar to that shown for flagellin (data not shown), suggesting that the EspA subunit has the potential to fold up as a "mini-flagellin" with lateral intersubunit interactions likely to be involved in EspA polymerization. Yip et al. (27) suggested that the central channel of EspA is wide enough to accommodate the passage of a folded EspA subunit. Indeed, it seems logical to suggest that EspA is maintained in an "assembly-competent" conformation which ensures rapid and efficient formation of the EspA filament upon protein secretion.

This project was supported by the Wellcome Trust.

REFERENCES

1. **Collington, G. K., I. W. Booth, and S. Knutton.** 1998. Rapid modulation of electrolyte transport in Caco-2 cell monolayers by enteropathogenic *Escherichia coli* (EPEC) infection. Gut **42:**200–207.
2. **Cravioto, A., R. J. Gross, S. M. Scotland, and B. Rowe.** 1979. An adhesive factor found in strains of *Escherichia coli* belonging to the traditional infantile enteropathogenic serogroups. Curr. Microbiol. **3:**95–99.
3. **Creasey, E. A., D. Friedberg, R. K. Shaw, T. Umanski, S. Knutton, I. Rosenshine, and G. Frankel.** 2003. CesAB is an enteropathogenic *Escherichia coli* chaperone for the type-III translocator proteins EspA and EspB. Microbiology **149:**3639–3647.
4. **Crepin, V. F., R. Shaw, C. M. Abe, S. Knutton, and G. Frankel.** 2005. Polarity of enteropathogenic *Escherichia coli* EspA filament assembly and protein secretion. J. Bacteriol. **187:**2881–2889.
5. **Crepin, V. F., R. Shaw, S. Knutton, and G. Frankel.** 2005. Molecular basis of antigenic polymorphism of EspA filaments: development of a peptide display technology. J. Mol. Biol. **350:**42–52.
6. **Daniell, S. J., E. Kocsis, E. Morris, S. Knutton, F. P. Booy, and G. Frankel.** 2003. 3D structure of EspA filaments from enteropathogenic *Escherichia coli*. Mol. Microbiol. **49:**301–308.
7. **Daniell, S. J., N. Takahashi, R. Wilson, D. Friedberg, I. Rosenshine, F. P. Booy, R. K. Shaw, S. Knutton, G. Frankel, and S. Aizawa.** 2001. The filamentous type III secretion translocon of enteropathogenic *Escherichia coli*. Cell. Microbiol. **3:**865–871.
8. **Delahay, R. M., S. Knutton, R. K. Shaw, E. L. Hartland, M. J. Pallen, and G. Frankel.** 1999. The coiled-coil domain of EspA is essential for the assembly of the type III secretion translocon on the surface of enteropathogenic *E. coli*. J. Biol. Chem. **274:**35969–35974.
9. **Dreyfus, G., A. W. Williams, I. Kawagishi, and R. M. Macnab.** 1993. Genetic and biochemical analysis of *Salmonella typhimurium* FliI, a flagellar protein related to the catalytic subunit of the F_0F_1 ATPase and to virulence proteins of mammalian and plant pathogens. J. Bacteriol. **175:**3131–3138.
10. **Galan, J. E., and H. Wolf-Watz.** 2006. Protein delivery into eukaryotic cells by type III secretion machines. Nature **444:**567–573.
11. **Garmendia, J., G. Frankel, and V. F. Crepin.** 2005. Enteropathogenic and enterohemorrhagic *Escherichia coli* infections: translocation, translocation, translocation. Infect. Immun. **73:**2573–2585.
12. **Kaper, J. B., J. P. Nataro, and H. L. Mobley.** 2004. Pathogenic *Escherichia coli*. Nat. Rev. Microbiol. **2:**123–140.
13. **Kenny, B., L. C. Lai, B. B. Finlay, and M. S. Donnenberg.** 1996. EspA, a protein secreted by enteropathogenic *Escherichia coli*, is required to induce signals in epithelial cells. Mol. Microbiol. **20:**313–323.
14. **Knutton, S., T. Baldwin, P. H. Williams, and A. S. McNeish.** 1989. Actin accumulation at sites of bacterial adhesion to tissue culture cells: basis of a new diagnostic test for enteropathogenic and enterohemorrhagic *Escherichia coli*. Infect. Immun. **57:**1290–1298.
15. **Knutton, S., D. R. Lloyd, and A. S. McNeish.** 1987. Adhesion of enteropathogenic *Escherichia coli* to human intestinal enterocytes and cultured human intestinal mucosa. Infect. Immun. **55:**69–77.
16. **Knutton, S., I. Rosenshine, M. J. Pallen, I. Nisan, B. C. Neves, C. Bain, C. Wolff, G. Dougan, and G. Frankel.** 1998. A novel EspA-associated surface organelle of enteropathogenic *Escherichia coli* involved in protein translocation into epithelial cells. EMBO J. **17:**2166–2176.
17. **Levine, M. M., E. J. Bergquist, D. R. Nalin, D. H. Waterman, R. B. Hornick, C. R. Young, and S. Sotman.** 1978. *Escherichia coli* strains that cause diarrhoea but do not produce heat-labile or heat-stable enterotoxins and are non-invasive. Lancet **i:**1119–1122.
18. **Lupas, A., M. Van Dyke, and J. Stock.** 1991. Predicting coiled coils from protein sequences. Science **252:**1162–1164.
19. **Macnab, R. M.** 2004. Type III flagellar protein export and flagellar assembly. Biochim. Biophys. Acta **1694:**207–217.
20. **McDaniel, T. K., K. G. Jarvis, M. S. Donnenberg, and J. B. Kaper.** 1995. A genetic locus of enterocyte effacement conserved among diverse enterobacterial pathogens. Proc. Natl. Acad. Sci. USA **92:**1664–1668.
21. **Mimori-Kiyosue, Y., F. Vonderviszt, I. Yamashita, Y. Fujiyoshi, and K. Namba.** 1996. Direct interaction of flagellin termini essential for polymorphic ability of flagellar filament. Proc. Natl. Acad. Sci. USA **93:**15108–15113.
22. **Mundy, R., T. T. MacDonald, G. Dougan, G. Frankel, and S. Wiles.** 2005. *Citrobacter rodentium* of mice and man. Cell. Microbiol. **7:**1697–1706.
23. **Pallen, M. J., S. A. Beatson, and C. M. Bailey.** 2005. Bioinformatics analysis of the locus for enterocyte effacement provides novel insights into type-III secretion. BMC Microbiol. **5:**9.
24. **Pallen, M. J., S. A. Beatson, and C. M. Bailey.** 2005. Bioinformatics, genomics and evolution of non-flagellar type-III secretion systems: a Darwinian perspective. FEMS Microbiol. Rev. **29:**201–229.
25. **Schlosser-Silverman, E., M. Elgrably-Weiss, I. Rosenshine, R. Kohen, and S. Altuvia.** 2000. Characterization of *Escherichia coli* DNA lesions generated within J774 macrophages. J. Bacteriol. **182:**5225–5230.
26. **Simpson, N., R. Shaw, R. Mundy, V. Crepin, A. J. FitzGerald, N. Cummings, I. Connerton, S. Knutton, and G. Frankel.** 2006. The enteropathogenic *E. coli* type III secretion system effector Map binds EBP50/NHERF1: implication for cell signalling and diarrhoea. Mol. Microbiol. **60:**349–363.
27. **Yip, C. K., B. B. Finlay, and N. C. Strynadka.** 2005. Structural characterization of a type III secretion system filament protein in complex with its chaperone. Nat. Struct. Mol. Biol. **12:**75–81.
28. **Yonekura, K., S. Maki-Yonekura, and K. Namba.** 2003. Complete atomic model of the bacterial flagellar filament by electron cryomicroscopy. Nature **424:**643–665.
29. **Yonekura, K., S. Maki-Yonekura, and K. Namba.** 2002. Growth mechanism of the bacterial flagellar filament. Res. Microbiol. **153:**191–197.

Downloaded from http://jb.asm.org/ on May 15, 2021 by guest